Effect of the Addition of Acrylonitrile/Ethylene–Propylene–Diene Monomer (EPDM)/Styrene Graft Copolymer on the Morphology–Properties Relationships in Poly(styrene-*co*-acrylonitrile)/EPDM Rubber Blends

Xiongwei Qu, Shurui Shang, Guodong Liu, Shengwen Zhang, Yan Zhang, Liucheng Zhang

Institute of Polymer Science and Engineering, School of Chemical Engineering, Hebei University of Technology, Tianjin, 300130, China

ABSTRACT: Blends of poly(styrene-*co*-acylonitrile) (SAN) with ethylene–propylene–diene monomer (EPDM) rubber were investigated. An improved toughness–stiffness balance of the SAN/EPDM blend was obtained when an appropriate amount of acrylonitrile–EPDM–styrene (AES) graft copolymer was added, prepared by grafting EPDM with styrene–acrylonitrile copolymer, and mixed thoroughly with both of the two components of the blend. Morphological observations indicated a finer dispersion of the EPDM particles in the SAN/EPDM/AES blends, and particle size distribution became narrower with increasing amounts of AES. Meanwhile, it was found that the SAN/EPDM blend having a ratio of 82.5/17.5 by weight was more effective in increasing the impact strength than that of the 90/10 blend. From dynamic mechanic analysis of the blends, the glass-transition temperature of the EPDM-rich phase increased from −53.9 to −46.2°C, even −32.0°C, for the ratio of 82.5/17.5 blend of SAN/EPDM, whereas that of the SAN-rich phase decreased from 109.2 to 108.6 and 107.5°C with the additions of 6 and 10% AES copolymer contents, respectively. It was confirmed that AES graft copolymer is an efficient compatibilizer for SAN/EPDM blend. The compatibilizer plays an important role in connecting two phases and improving the stress transfer in the blends. Certain morphological features such as thin filament connecting and even networking of the dispersed rubber phase may contribute to the overall ductility of the high impact strength of the studied blends. Moreover, its potential to induce a brittle–ductile transition of the glassy SAN matrix is considered to explain the toughening mechanism. © 2003 Wiley Periodicals, Inc. J Appl Polym Sci 91: 1685–1697, 2004

Key words: compatibility; graft copolymers; blends; structure–property relations; morphology

INTRODUCTION

The acrylonitrile–butadiene–styrene (ABS) copolymer is one of the most commonly used engineering plastics because of its high impact strength[1,2] and has been used in fused deposition manufacturing (FDM) technology.[3] FDM, a new kind of rapid prototyping modeling in mechanical manufacturing, can be used to shorten the producing cycle, correct the error in designing, and decrease the production cost. Some requirements of FDM filament materials for this technology are as follows: (1) high tensile strength and compression strength for the input of capillary, (2) high thermal stability for high molding temperature, and (3) high melt flow and good adhesion between two layers. Even ABS has been used in FDM technology; it has poor thermal stability for the polybutadiene (PB) component. Among the several attempts to improve the poor performances, the substitution of the ethylene–propylene–diene monomer (EPDM) rubber for polybutadiene has been widely investigated[4–6] because it is known that EPDM has outstanding resistance to heat, light, oxygen, and ozone attributed to its nonconjugated diene component.

Blending of acrylonitrile–styrene copolymer (SAN) with EPDM rubber (SAN/EPDM) may provide an efficient way with tailored properties. Although SAN/EPDM system is a brittle/ductile combination, the blend does not result in a toughened plastic, given that the two components are immiscible at the molecular level because of their difference in polarity, and blends have poor mechanical properties compared to those of their net components. Therefore, the introduction of a small amount of compatibilizer has been investigated to obtain more desirable properties. Generally, an effective compatibilizer reduces the interfacial tension between the two phases and thus leads to

a decrease in the particle size and stabilizes the phase morphology against coalescence.[7–9] Grafting a styrene–acrylonitrile copolymer onto the EPDM rubber may provide the continuity of the two phases on the interface, which is indispensable for the blend to be applied to structural materials. The characteristics and thermal properties of graft copolymerization of styrene and acrylonitrile onto EPDM (AES) were previously reported.[10] In this study, we investigate the tensile strength, impact strength, and two-phase morphology of binary SAN/EPDM and ternary SAN/EPDM/AES blends. On the basis of the results, we show the importance of interfacial adhesion and morphological features for the toughening in these brittle/rubber polymer systems to have a practical use of this material in industry.

EXPERIMENTAL

Materials

SAN copolymer (PN-137H) was provided by Qimei Corp. (Taiwan). EPDM (4045) was made by Jilin Chemical Corp. (China). Acrylonitrile–EPDM–styrene (AES) graft copolymer was polymerized in our laboratory and the details of synthesis, separation, and characterization are given elsewhere.[10] The parameters of the grafting ratio and efficiency of the graft copolymer were 34.7 and 64.5%, respectively.

Blend preparation

All the polymers were dried under vacuum at 85°C for at least 12 h before blending. The polymers were blended in two-roll mixer at 165°C for 10 min, and injection-molded into dumbbell-shape samples. The compositions of SAN/EPDM blends were 90/10 and 82.5/17.5 by weight. These rubber concentrations were chosen to obtain a balance in toughness and tensile strength. The weight percentages of added AES graft copolymer with respect to the total weight of SAN/EPDM blend were 0, 1, 3, 6, 8, and 10%.

Morphological observations

Using a Philips XL-30 scanning electron microscope (SEM; Philips, The Netherlands), the morphology of fractured specimens was observed. The cryogenic specimens were dipped in liquid nitrogen for about 20 min and immediately fractured perpendicular to the mold flow direction. For better observation of the morphology, especially in ternary blends, the fractured specimens were etched selectively by immersion in n-hexane to remove the EPDM phase and coated with gold before viewing to avoid charging. The SEM micrographs were analyzed to determine the average particle size and particle size distribution of the dispersed EPDM phase by an image analyzer. The waddle diameter (diameter of a circle having equivalent area of a round shape) of each particle was computed. An average of 300 diameter measurements per sample was obtained. The number-average diameter (D_n) of dispersed EPDM particles was calculated from the following equation:

$$D_n = \frac{\sum N_i D_i}{\sum N_i}$$

where N_i is the number of particles having a diameter D_i.

The morphology of specimens after the impact test was examined without etching.

Transmission electron microscopy (TEM) measurements were done with a Hitachi H-800 transmission electron microscope (Hitachi, Ibaraki, Japan), applying an acceleration voltage of 80 kV. The samples were cut with an ultramicrotome at room temperature (liquid nitrogen). Ultrathin sections of about 70–100 nm were stained with RuO_4 or OsO_4 to obtain electron micrographs with excellent contrast and definition.

Impact and tensile testing

The Charpy notched impact tests on the specimens were carried out with a pendulum-type impact tester (CXJ-40; Chengde Testing Instruments, Chengde City, Hebei Province, China) at room temperature. At least five runs were made to report the average.

Tensile properties were measured on an Instron (model 1122; Instron, Canton, MA) tensile machine according to the ASTM D-638 standard procedure using a crosshead speed of 5 mm/min at room temperature.

Dynamic mechanical analysis

The measurement of dynamic mechanic analysis of the blends was carried out in a Netzsch 242 dynamic mechanic analyzer (DMA) (NETZSCH Feinmahltechnik GmbH, Selb, Germany) operated at a fixed frequency of 1 Hz. All experiments were carried out in the temperature range of −150 to 130°C at a heating rate of 3°C/min. The plots were processed by computer for the determination of the tan δ values.

RESULTS AND DISCUSSION

Morphology of cryogenically fractured surface

Electron microscopy can be used to determine the size and distribution of the rubber domains. The morphology of cryogenically fractured surface of SAN/EPDM blend is shown in Figure 1(a) and (b) for the ratios of 90/10 and 82.5/17.5 SAN/EPDM blends, respectively. Because of its pronounced incompatibility with polar
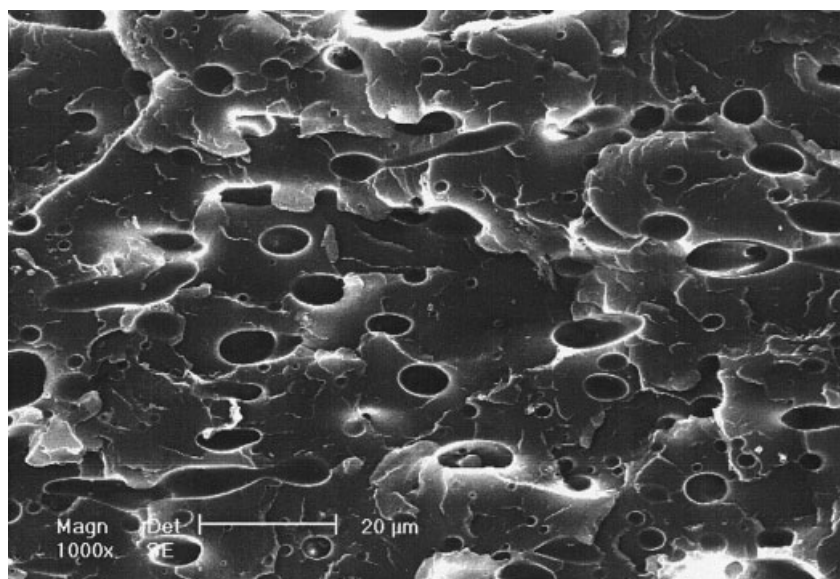
(a)
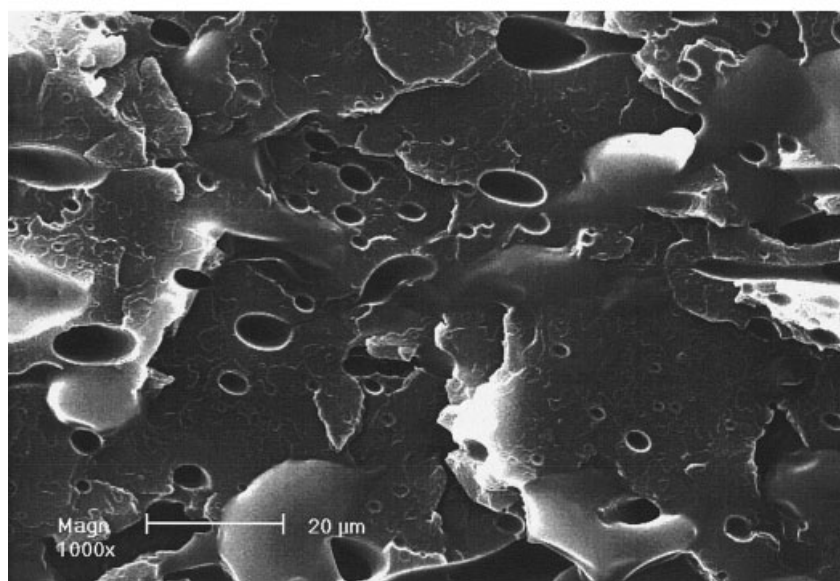
(b)

Figure 1 SEM micrographs of cryogenically fractured surfaces of SAN/EPDM blends (magnification ×1000): (a) 90/10; (b) 82.5/17.5.

polymers, as evident from their high values of interfacial tension,[11,12] EPDM requires a compatibilizer during melt processing in blends with SAN. Otherwise, the high interfacial tension between the different phases leads to a large size of the dispersed rubber phase, as shown in Figure 1.

In the absence of a common component, the immiscible phases will seek to minimize the extent of interpenetration across the interface by adopting more collapsed conformations in the immiscible vicinity of the interface. This is the primary cause of interfacial weakness in immiscible blends. The poor interface is attrib-

uted to the weak interfacial adhesion between SAN and EPDM.

Morphological changes of SAN/EPDM blends with the addition of AES graft copolymer are presented in Figures 2 and 3 for the ratios of 90/10 and 82.5/17.5 blends, respectively. For the ternary blends, the addition of AES graft copolymer results in a significant reduction of the dispersed EPDM phase. The graft composition of styrene to acrylonitrile was kept at the azeotropic point, which is the same as that of typical commercial SAN products.[13–16] Therefore, there was a high degree of compatibility between the SAN grafted
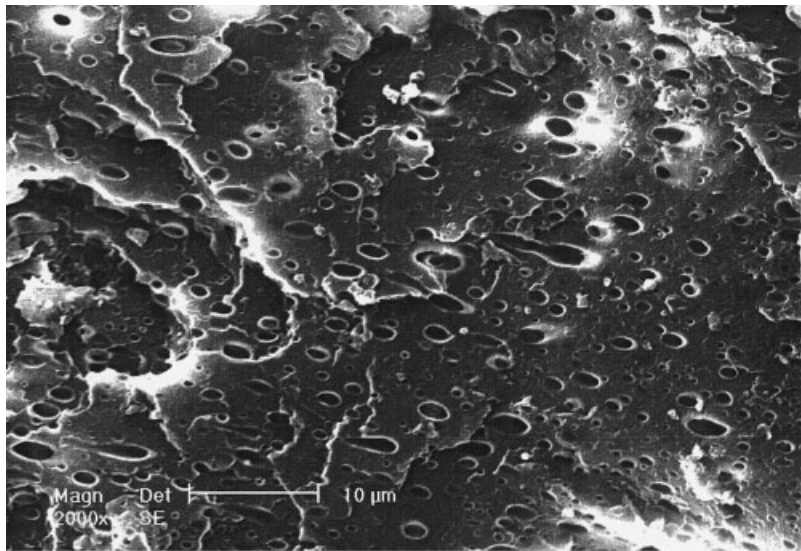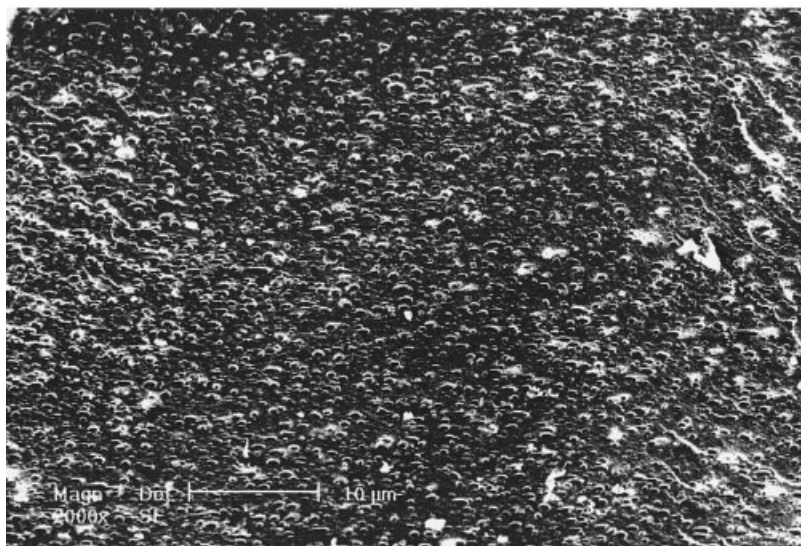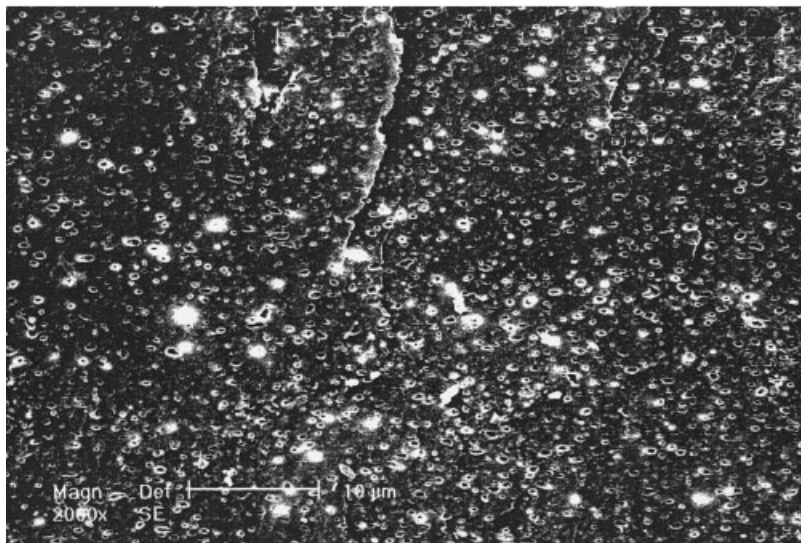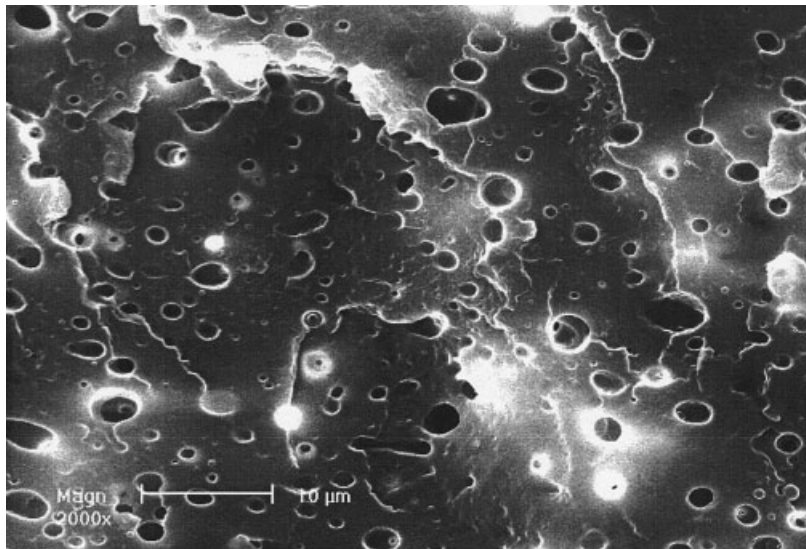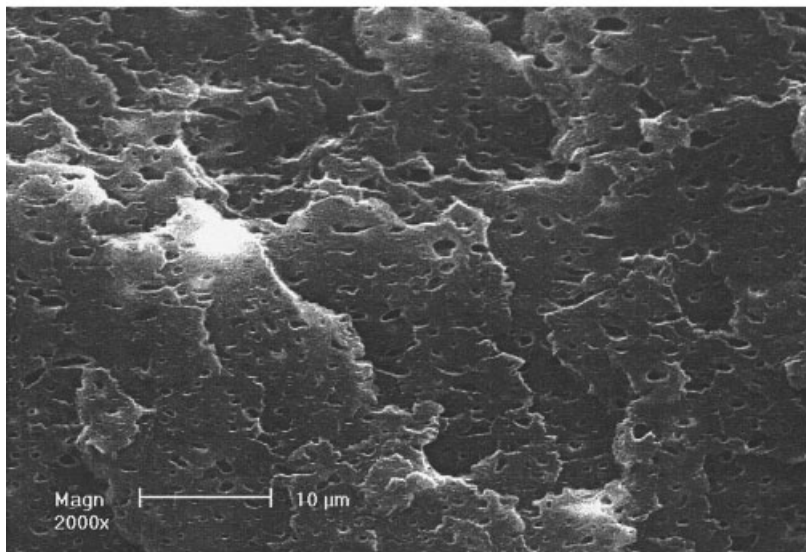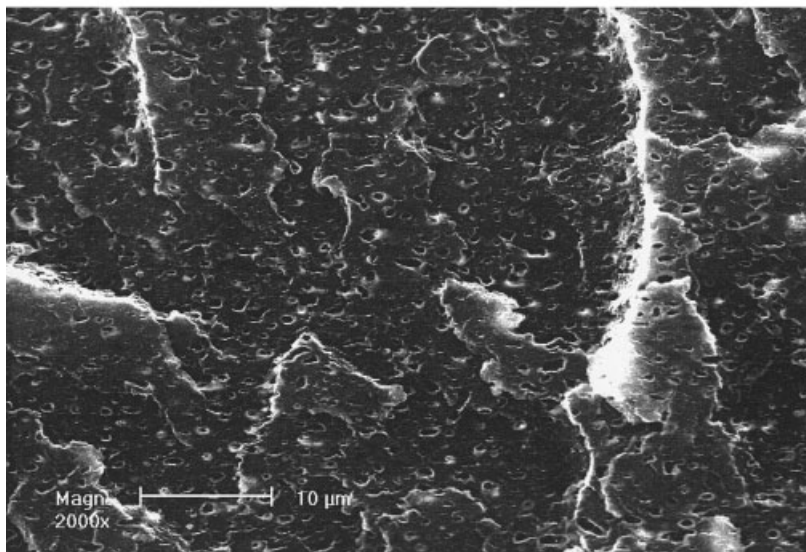
Figure 2 SEM micrographs of cryogenically fractured surfaces of SAN/EPDM/AES (90/10/AES) blends, where AES is (a) 1%; (b) 6%; (c) 10% (magnification ×2000).

Figure 3 SEM micrographs of cryogenically fractured surfaces of SAN/EPDM/AES (82.5/17.5/AES) blends, where AES is (a) 1%; (b) 6%; (c) 10% (magnification ×2000).
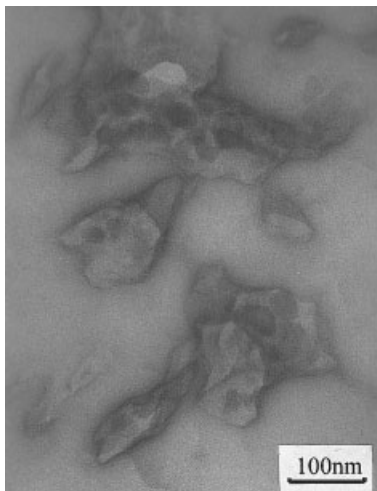
Figure 4 Transmission electron photomicrograph of RuO_4-stained ultrathin section of SAN/EPDM/AES (90/10/10) blend.

to the rubber particles and the matrix. In the presence of a common blend component, all of the blend constituents could attain additional freedom to adopt more favorable conformations in the vicinity of the interface.[17] This could occur if the common component was to become more enriched in the interfacial area and interpenetrate freely with each phase. Because of the stronger thermodynamic driving force for diffusion, adhesion develops most rapidly. Improved molecular interpenetration across the interface equates to better adhesion between the phases. The graft copolymer will preferentially locate at the interface between the two phases, thus reducing the interfacial tension and enhancing the adhesion between phases. As shown in Figure 2, the particle size decreases with the addition of AES because of the interfacial activity of AES graft copolymer produced during mechanical mixing. The reduction in interfacial tension with increasing graft copolymer concentration arose mainly from the energetically preferred orientation of the blocks at the interface into their respective compatible components. These performances also occur in 82.5/17.5 blends, as shown in Figure 3.

To study the morphology of the matrix/rubber interface, the ternary SAN/EPDM/AES (90/10/10) system was investigated using TEM. Figure 4 shows a portion of a TEM image, an ultrathin section stained by RuO_4. It may be observed that there is an obvious concentration gradient around the dispersed phase of EPDM. The interfaces between polymers are diffuse, as the segments of polymer chains interpenetrate to minimize the free energy, thus providing good evidence for the locating of AES at the SAN/EPDM interface, even at a low concentration of EPDM rubber.

The statistical results of the variation in number-average particle diameter of SAN/EPDM blends with

the amount of graft copolymer are plotted in Figure 5, which indicates that addition of 1% AES to the SAN/EPDM (82.5/17.5) blend causes a significant reduction of the dispersed rubber phase in the domain size from 3.20 to 1.26 μm by about 60%. Further addition of AES graft copolymer decreases the domain size continuously and levels off above 6%. This trend can also be seen in the 90/10 ratio blends. When AES graft copolymer content was increased to 10%, the EPDM rubber particle sizes of the two blends were nearly constant, which means that neither a further reduction nor coalescence of the particles occurred when there was a significant interface adhesion between the dispersion and the matrix phase.[18–20]

The effect of AES graft copolymer addition on particle size distribution of SAN/EPDM blends was also examined, as shown in Figure 6. The uncompatibilized blend shows a border distribution in particle size, as shown in Figure 6(a) and (e). When 1% of AES was added to both blends, the particle size distributions become narrower as evidenced by the decrease in the width of the distribution curve, as in Figure 6(b) and (f). This indicates that small amounts of AES are sufficient for effective compatibility. It has been also reported in the literature that the addition of a compatibilizer to immiscible polymer blends not only reduces the size of the minor phase, but also results in uniform size distribution.[9,16,18,21,22]

Mechanical properties of the blends and electronic micrograph observation of the impact fracture surfaces

The effect of graft copolymer addition on the impact strength of different compositions of SAN/EPDM
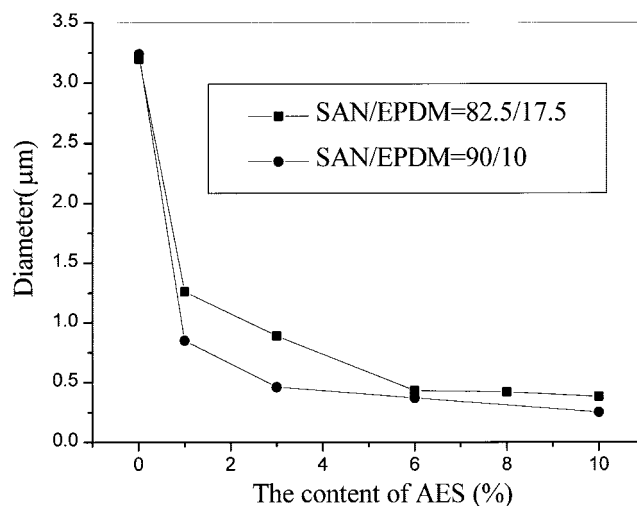

Figure 5 Number-average diameter (D_n) of dispersed EPDM particles versus content of AES graft copolymer in SAN/EPDM blends. Circles and squares indicate SAN/EPDM blends of 90/10 and 82.5/17.5, respectively.
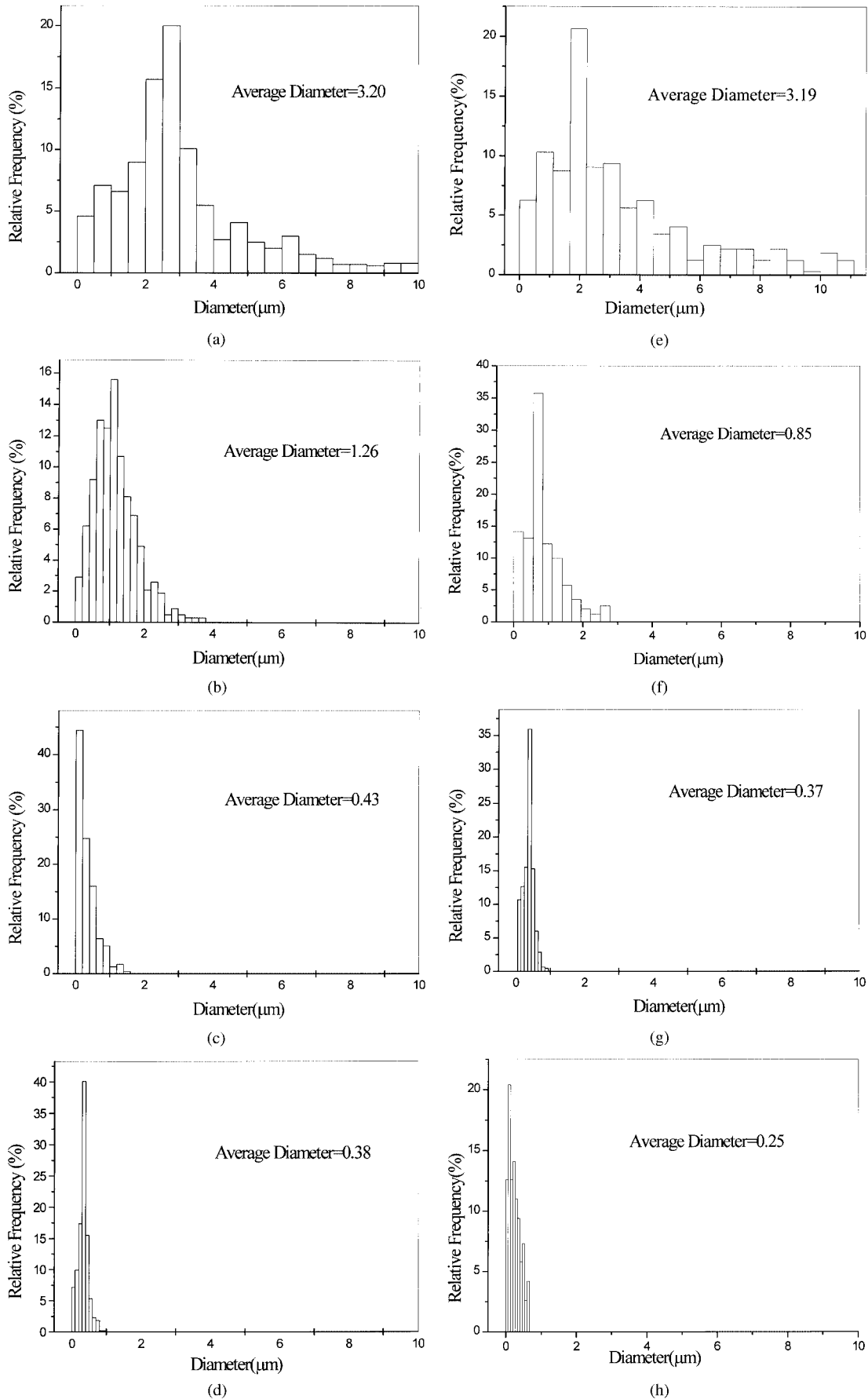
Figure 6 Particle size distribution of dispersed EPDM phase for SAN/EPDM/AES blends: (a) 82.5/17.5/0; (b) 82.5/17.5/1; (c) 82.5/17.5/6; (d) 82.5/17.5/10; (e) 90/10/0; (f) 90/10/1; (g) 90/10/6; (h) 90/10/10.
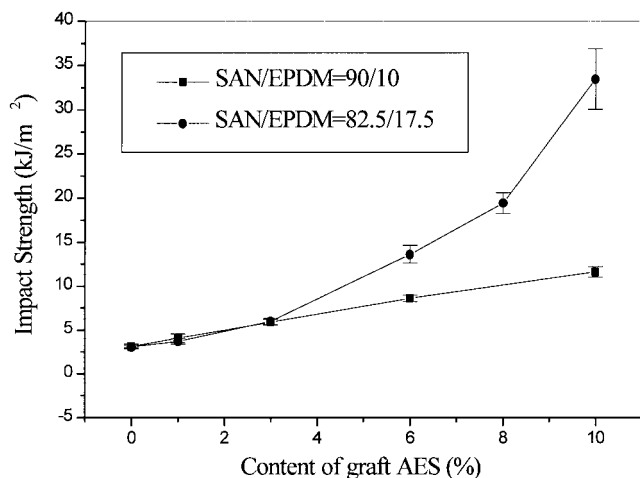
Figure 7 Impact strength versus content of graft copolymer for SAN/EPDM blends. Squares and circles indicate the blends of 90/10 and 82.5/17.5, respectively.

blends was investigated. As shown in Figure 7, the impact strength of the 82.5/17.5 blend compatibilized with the addition of 10% AES graft copolymer increases by ten times higher than that without graft copolymer, whereas that of 90/10 blends increases only 1.5 times at the same content of compatibilizer. A brittle–tough transition in the impact strength was observed only at a composition of about 17.5 wt % EPDM. For the SAN/EPDM (90/10) system, a gradual increase in impact strength was observed with increasing AES content, although the effect was small compared with the transition. In other words, the ternary blends of 82.5/17.5/AES systems exhibit much higher impact strength than those of the 90/10/AES system when adding the same content of AES. The improved toughness in SAN/EPDM/AES blends clearly indicates that AES is able to act as a compatibilizer. In the present SAN/EPDM/AES systems, the ability of AES to migrate to the interface between EPDM and SAN is identical, as shown in Figure 4. Thus, the toughening mechanism might be related to the difference of the EPDM morphology.

According to Wu's classification,[23,24] including entanglement density and characteristic ratio of the chain, SAN should be classified as a brittle polymer. Under ordinary conditions, SAN/rubber blends tend to fail by crazing or mixed crazing and yielding.[23] Some authors suggested that bimodal-size (i.e., mixtures of distinctly large and small) rubber particles had a pronounced synergistic toughening effect in SAN.[25,26]

Ultrathin sections of injection-molded specimens were examined by TEM for selected blends having major differences in ductility. Figure 8 shows 10 and 17.5% rubber levels in the SAN matrix polymers containing 10% compatibilizer. All electron micrographs

of sections were positive, where the osmium-stained rubber phase appears dark against the brighter SAN resin matrix. Figure 8(a) reveals thin filaments connecting some of the particles in the 10% rubber content blend. It is particularly noticeable with 17.5% rubber content, from the high-magnification photomicrographs that the SAN/EPDM/AES (82.5/17.5/10) blend shows a special morphology of cocontinuous structure with a satisfactory level of adhesion, shown in Figure 8(b). It appears that these connected particles may be capable of craze initiation in some of the blends studied here. Crazes may be terminated at shear bands that are initiated by individual small particles or by mutual termination of several crazes, where the relative rubber concentration is high.[27] Meanwhile, flocculation to form an interconnected rubber–particle network is much more beneficial to
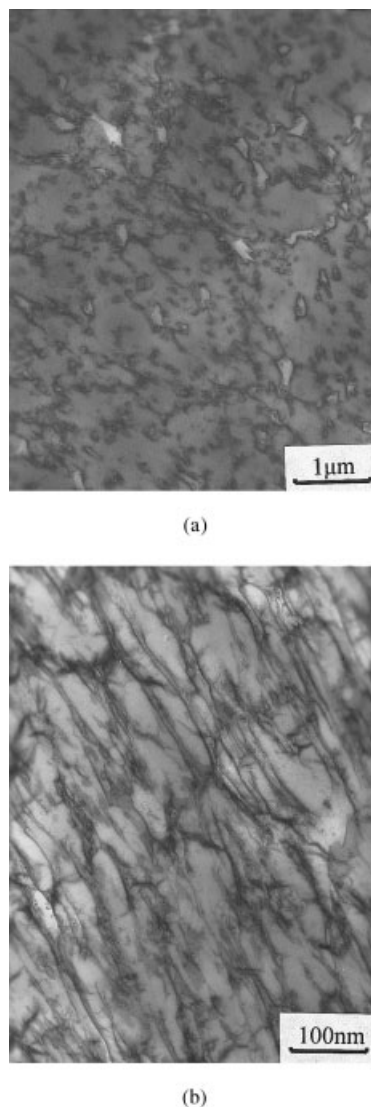

(a)

(b)

Figure 8 Transmission electron photomicrograph of OsO$_4$-stained ultrathin section of SAN/EPDM/AES blend: (a) 90/10/10; (b) 82.5/17.5/10.
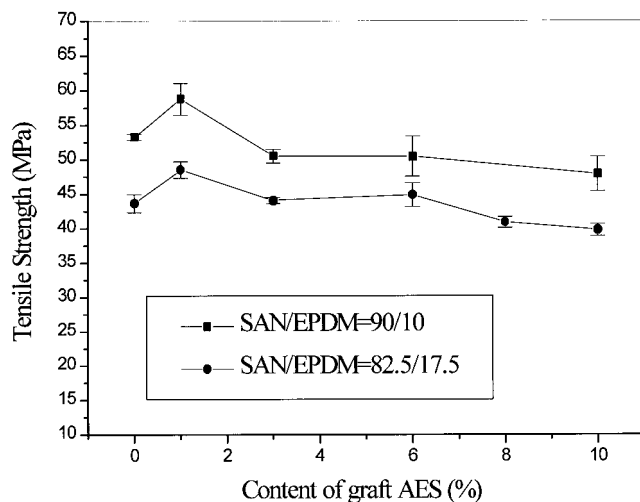
Figure 9 Effect of AES contents on tensile strength of SAN/EPDM blends.

toughening.[23] Asymmetrical particles such as ribbons and networks are more effective than spheroidal ones. It may also be possible that a high concentration of small particles at the craze tip may interact with the growing craze stress field impeding its further progress. Thus, this network formation may contribute to the ductility and toughness of the EPDM/SAN/AES (82.5/17.5/10) blends described here.

Taking into account the above-mentioned results, it seems that the toughening of SAN/EPDM (82.5/17.5 composition) by incorporation of 10% AES graft copolymer does not result from rubber particle size reduction but from the change of morphological structures.

The tensile strength is an important characteristic of polymeric materials because it indicates the limit of final stress in most applications. The tensile strength of these ternary blends is almost independent of the added amount of AES, as shown in Figure 9. The much smaller decrease represents the existence of an interface region by which two phases are bonded strongly because the tensile strength is strongly dependent on the interface structure of the blends. The stress has to transfer across the interface to avoid the fracture.

Meier and Inoue and Hong previously showed that the thickness of the interface between A and B polymer phases increased with the addition of A–B block or graft polymers.[28] Strong interactions result in good adhesion and efficient stress transfer from the continuous to the dispersed polymer phase in the blends. Therefore, an improved toughness–stiffness balance may be obtained in SAN/EPDM blends by adding AES graft copolymer.

Morphology of the fractured surface of the uncompatibilized SAN/EPDM blend after impact testing is shown in Figure 10(a) and (b). The fractured surfaces

of the 90/10 and 82.5/17.5 ratio blends exhibit typical morphologies of blends with low impact strength: relatively smooth and the troughs are clear and the particles are easily pulled out, implying a poor adhesion between SAN and EPDM rubber. Figure 11 shows a variation in morphology of fractured surfaces of SAN/EPDM/AES (82.5/17.5/AES) blends after impact testing as a function of AES copolymer contents. As the amount of AES increases, the fractured surface of the blends becomes rougher. In Figure 11(c), SEM photomicrographs of the fracture surfaces show extensive matrix yielding, characteristic of toughness failure. No rubber particles are visible on the fracture surface. Figure 12 shows SEM micrographs of fractured surfaces of SAN/EPDM/AES (90/10/AES) blends after impact testing. The change of the fractured section is not so obvious as that of the 82.5/17.5/10 ratio blends, which show little matrix yielding and break in a brittle fashion. The materials showing less ductile behavior have more irregular surfaces, whereas the toughest blends show a rather homogeneous surface. The surfaces of the tough blends show indications of plastic flow during the fracture process not observed with more brittle blends. These photomicrographs are quite consistent with the increase in toughness observed by adding 17.5% rubber content to the SAN matrix.

Dynamic mechanical analysis of the blends

Measurements of the glass-transition temperatures (T_g) were used to study the miscibility of SAN/EPDM systems because the difference in the T_g values of EPDM and SAN was sufficiently large. The T_g values were measured by dynamic mechanical analysis. Plots of tan δ against temperature were used to measure T_g values, assigned to the maximum of tan δ. The results are given in Figure 13 for the ratio of 82.5/17.5 blends with varying AES graft copolymer content. Curve (a) shows two separate tan δ peaks of the SAN/EPDM blend at temperatures of −53.9 and 109.2°C, corresponding to the EPDM-rich phase and the SAN-rich phase, respectively. As some of AES graft copolymer is added to the SAN/EPDM blends, the tan δ peak of the SAN-rich phase shifts to 107.5°C [Fig. 13(c)], a lower temperature after addition of 10% AES copolymer, whereas that of the EPDM-rich phase moves to −46.2 and −32.0°C [Fig. 13(b), (c)], significantly higher values, at AES contents of 6 and 10%, respectively. Meanwhile, the curves shown in Figure 13 do not reveal a new peak. This means that a new isolated phase in SAN/EPDM/AES ternary blends does not form, and AES graft copolymer locates at the boundary between SAN and EPDM. Besides, the widths of the peaks are the same as those of neat polymers, SAN and EPDM. This result also supports the increasing
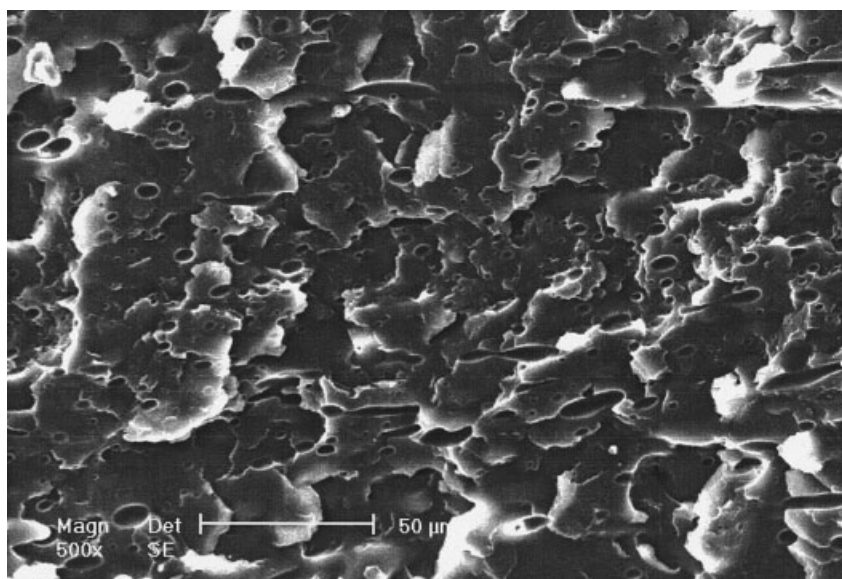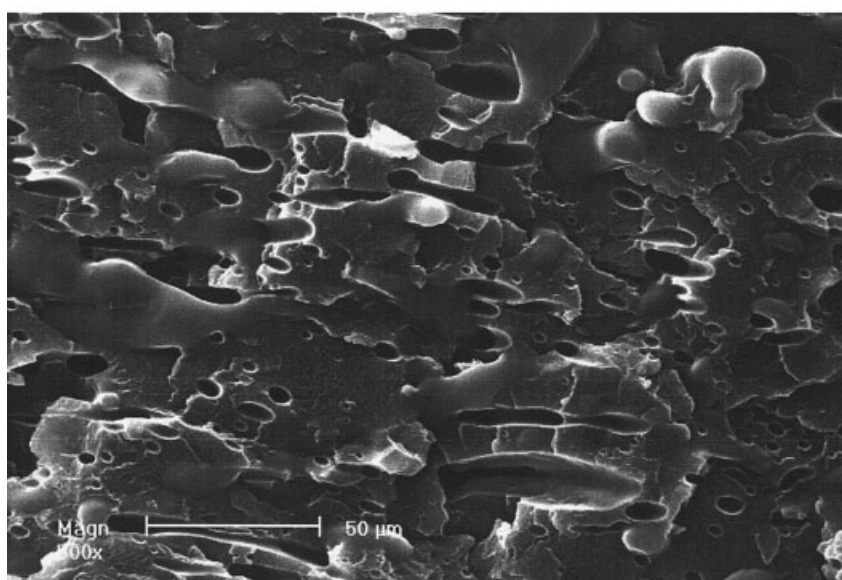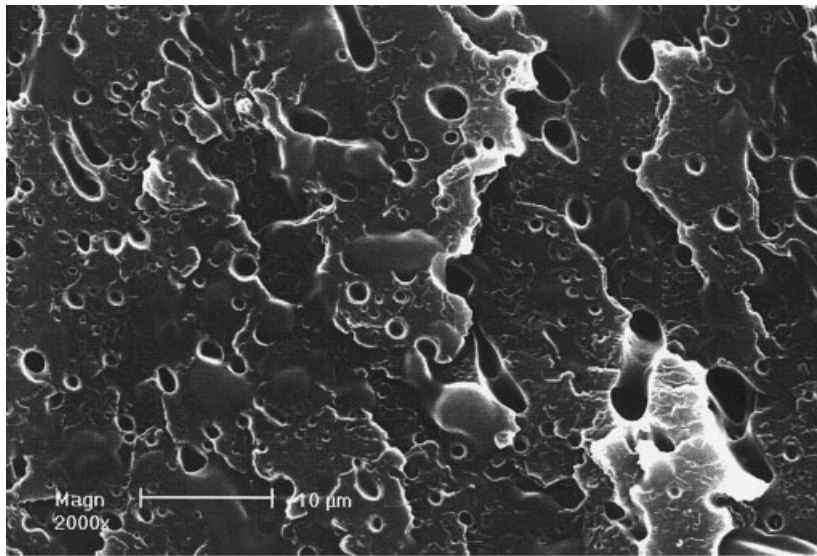
Figure 10 SEM micrographs of fractured surfaces of uncompatibilized SAN/EPDM blends after impact test: (a) 90/10; (b) 82.5/17.5.

compatibility between SAN and EPDM rubber with the addition of AES graft copolymer.

CONCLUSIONS

On the basis of the results, including the tensile properties, impact strength, and two-phase morphology of binary SAN/EPDM and ternary SAN/EPDM/AES blends, we have shown that AES is able to act as a compatibilizer in SAN/EPDM blends. Small amounts of AES are sufficient to achieve a finer dispersion of the EPDM rubber phase and the particle size distribu-

tion is narrowed. Further addition leaves the morphology unchanged, but impact properties are significantly improved upon addition up to 10% of AES with the stiffness retained. The blend containing 17.5% of rubber exhibits better impact properties than the blend with a 10% rubber fraction. Furthermore, a significant increase of the glass-transition temperature of the dispersed rubber phase can be observed from the results of dynamic mechanical analysis, indicating the good compatibility and adhesion between SAN and EPDM rubber. It is suggested that the small monodisperse EPDM phase proves to be an effective toughen-
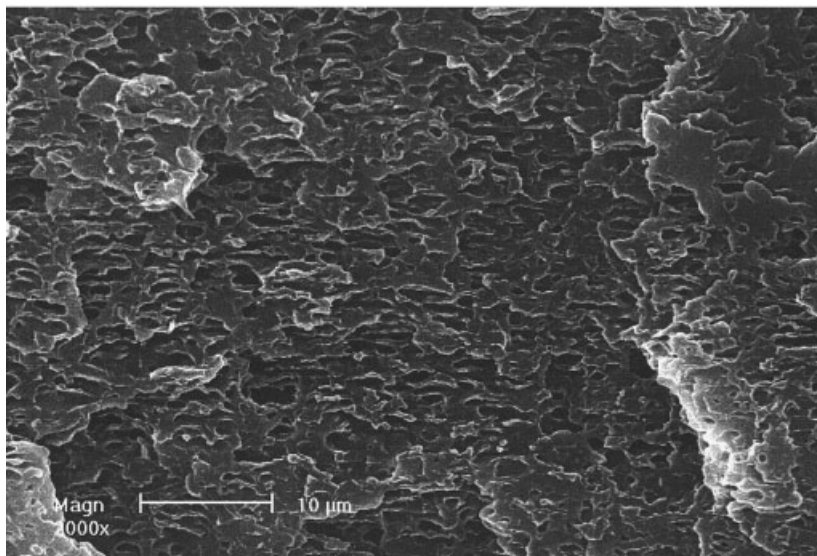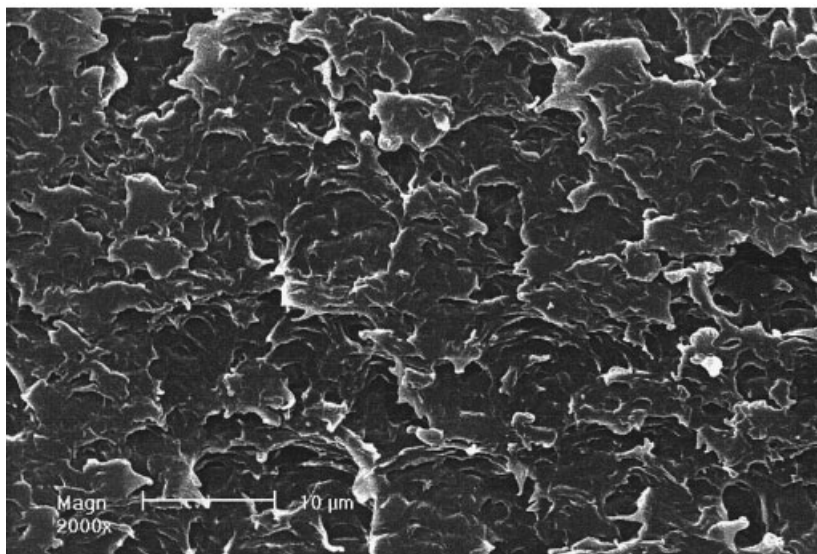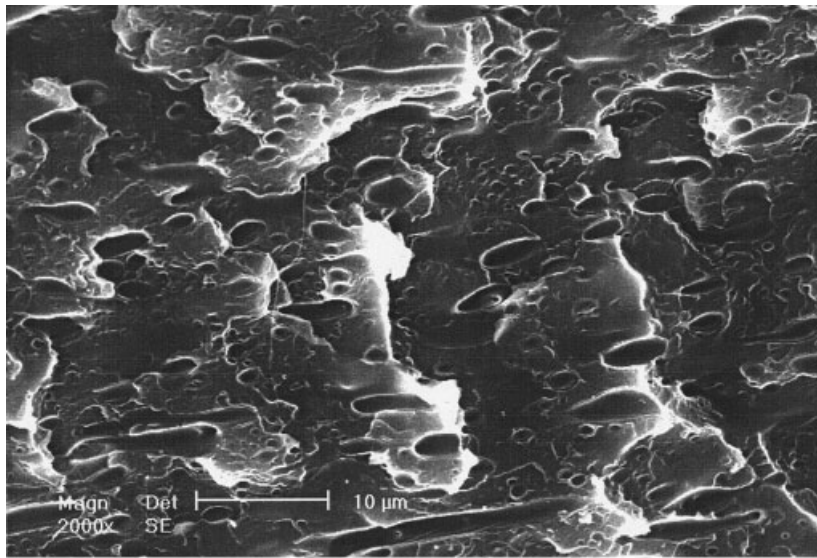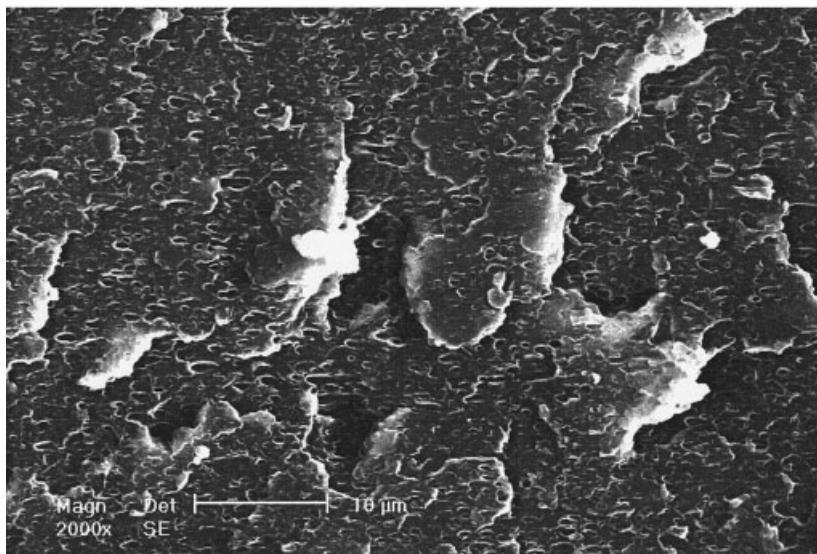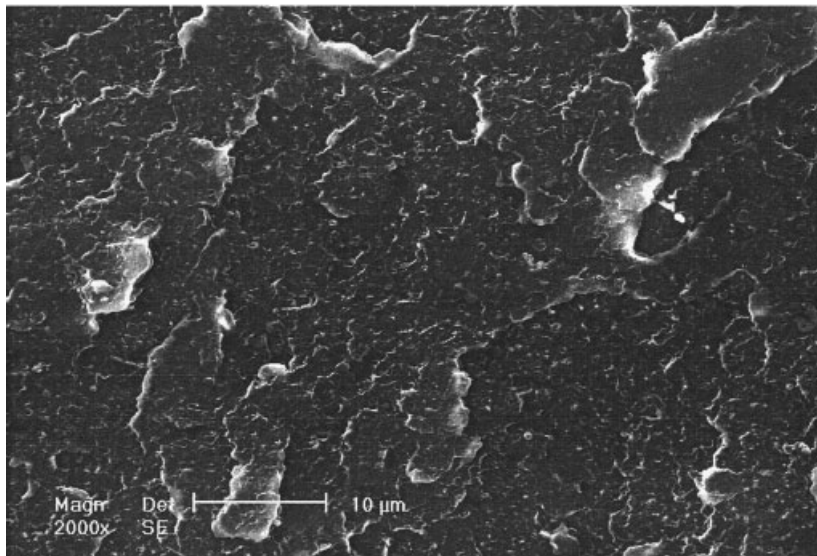
Figure 11 SEM micrographs of fractured surfaces of SAN/EPDM/AES (82.5/17.5/AES) blends after impact test, where AES is (a) 1%; (b) 6%; (c) 10% (magnification ×2000).

Figure 12 SEM micrographs of fractured surfaces of SAN/EPDM/AES (90/10/AES) blends after impact test, where AES is (a) 1%; (b) 6%; (c) 10% (magnification ×2000).
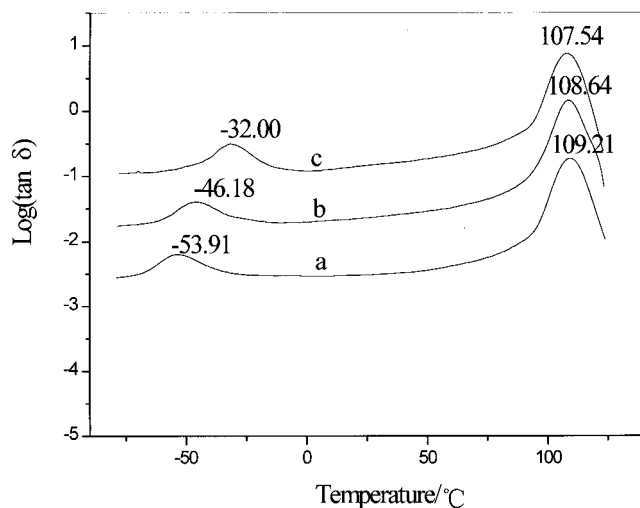
Figure 13 Dynamic mechanical graphs of SAN/EPDM/ AES blends: (a) SAN/EPDM = 82.5/17.5; (b) SAN/EPDM/ AES = 82.5/17.5/6; (c) SAN/EPDM/AES = 82.5/17.5/10.

ing agent for the commercial SAN copolymer with the addition of AES graft copolymer without the presence of larger rubber particles.

References

1. Kulich, D. M.; Kelley, P. D.; Pace, J. E. In: Encyclopedia of Polymer Science and Engineering, 2nd ed.; Kroschwitz, J. I., Ed.; Wiley: New York, 1985; Vol. 1, p. 388.
2. Bae, Y. O.; Ha, C. S.; Cuo, W. J. Eur Polym Sci 1991, 27, 121.
3. Wu, L.; Hong, G.; Wu, R.; Yan, Y.; Zhang, Z. In: Proceedings of the First International Conference on Rapid Prototyping and Manufacturing, Beijing, July 1998; Yan, Y., Ed.; Shaanxi Science and Technology: Xi'an, 1998; p. 159.
4. Meredith, C. L.; von Bodungen, G. A. U.S. Pat. 3,657,395, 1972.
5. Morimoto, M. J Appl Polym Sci 1981, 26, 261.
6. Castellani, L.; Lomellini, P. Plast Rubber Compos Process Appl 1991, 16, 25.
7. Adedeji, A.; Jamieson, A. M.; Hudson, S. D. Macromolecules 1994, 27, 4018.
8. Adedeji, A.; Hudson, S. D.; Jamieson, A. M. Macromolecules 1996, 29, 2449.
9. Cowie, J. M. G.; Ferguson, R.; McEwen, I. J.; Reid, V. M. C. Polymer 1994, 35, 1473.
10. Qu, X.; Shang, S.; Liu, G.; Zhang, L. J Appl Polym Sci 2002, 86, 428.
11. Schoolenberg, G. E.; During, F. Polymer 1998, 39, 757.
12. Schoolenberg, G. E.; During, F.; Ingenbleek, G. Polymer 1998, 39, 765.
13. Schwarz, M. C.; Barlow, J. W.; Paul, D. R. J Appl Polym Sci 1989, 37, 403.
14. Kim, H.; Keskkula, H.; Paul, D. R. Polymer 1990, 31, 869.
15. Hachiya, H.; Takayama, S.; Takeda, K. J Appl Polym Sci 1998, 70, 2521.
16. Hwang, I. J.; Kim, B. K. J Appl Polym Sci 1998, 67, 27.
17. Machado, J. M.; Lee, C. S. Polym Eng Sci 1994, 34, 59.
18. Hong, B. K.; Jo, W. H. Polymer 2000, 41, 2069.
19. Angola, J. C.; Fujita, Y.; Sakai, T.; Inoue, T. J Polym Sci Part B: Polym Phys 1988, 26, 807.
20. Mader, D.; Kressler, J.; Mulhaupt, R. J Appl Polym Sci 1999, 73, 1685.
21. Shaw, S.; Singh, R. P. Eur Polym J 1989, 25, 445.
22. Mader, D.; Kressler, J.; Mulhaupt, R. J Appl Polym Sci 1999, 73, 1685.
23. Wu, S. Polym Eng Sci 1990, 30, 753.
24. Wu, S. Polym Int 1992, 29, 229.
25. Fowler, M. E.; Keskkula, H.; Paul, D. R. Polymer 1987, 28, 1703.
26. Fowler, M. E.; Keskkula, H.; Paul, D. R. J Appl Polym Sci 1988, 35, 1563.
27. Keskkula, H.; Kim, H.; Paul, D. R. Polym Eng Sci 1990, 30, 1373.
28. Noolandi, J.; Hong, K. M. Macromolecules 1984, 17, 1531.